Bioorganic & Medicinal Chemistry 19 (2011) 3416–3424

Contents lists available at ScienceDirect

Bioorganic & Medicinal Chemistry

journal homepage: www.elsevier.com/locate/bmc

Design, synthesis, and biological evaluation of substituted hydrazone and pyrazole derivatives as selective COX-2 inhibitors: Molecular docking study

Magda A.-A. El-Sayed [a], Naglaa I. Abdel-Aziz [b,*], Alaa A.-M. Abdel-Aziz [b,c], Adel S. El-Azab [c,d], Yousif A. Asiri [e], Kamal E. H. ElTahir [f]

[a] Department of Pharmaceutical Organic Chemistry, Faculty of Pharmacy, University of Mansoura, Mansoura 35516, Egypt
[b] Department of Medicinal Chemistry, Faculty of Pharmacy, University of Mansoura, Mansoura 35516, Egypt
[c] Department of Pharmaceutical Chemistry, College of Pharmacy, King Saud University, Riyadh 11451, Saudi Arabia
[d] Department of Organic Chemistry, Faculty of Pharmacy, Al-Azhar University, Cairo, Egypt
[e] Department of Clinical Pharmacy, College of Pharmacy, King Saud University, Riyadh 11451, Saudi Arabia
[f] Department of Pharmacology, College of Pharmacy, King Saud University, Riyadh 11451, Saudi Arabia

ARTICLE INFO

Article history:
Received 3 February 2011
Revised 12 April 2011
Accepted 13 April 2011
Available online 22 April 2011

Keywords:
Hydrazone and pyrazole derivatives
Selective COX-2 inhibitors
Molecular docking

ABSTRACT

New arylhydrazone derivatives and a series of 1,5-diphenyl pyrazoles were designed and synthesized from 1-(4-chlorophenyl)-4,4,4-trifuorobutane-1,3-dione **1**. The newly synthesized compounds were investigated in vivo for their anti-inflammatory activities using carrageenan-induced rat paw oedema model. Moreover, they were tested for their inhibitory activity against ovine COX-1 and COX-2 using an in vitro cyclooxygenase (COX) inhibition assay. Some of the new compounds (**2f**, **6a** and **6d**) showed a reasonable in vitro COX-2 inhibitory activity, with IC_{50} value of 0.45 μM and selectivity index of 111.1. A virtual screening was carried out through docking the designed compounds into the COX-2 binding site to predict if these compounds have analogous binding mode to the COX-2 inhibitors. Docking study of the synthesized compounds **2f**, **6a** and **6d** into the active site of COX-2 revealed a similar binding mode to SC-558, a selective COX-2 inhibitor.

1. Introduction

Cyclooxygenase is the key enzyme in the biosynthesis of prostanoids, biologically active substances that are involved in several physiological processes but also in pathological conditions, such as inflammation.[1] It is actually well-known that this enzyme exists under two forms: cyclooxygenase-1 (COX-1) and cyclooxygenase-2 (COX-2). COX-1 is a constitutive enzyme and is responsible for the production of cytoprotective prostaglandins in the gastrointestinal tract (GI) and proaggregatory thromboxane in blood platelets. However, COX-2 is an inducible enzyme which is induced in response to the release of several proinflammatory mediators.[2–4] Both enzymes are sensitive to inhibition by conventional non-steroidal anti-inflammatory drugs (NSAIDs). Observations that COX-1 was involved in several homeostatic processes, while COX-2 expression was associated with inflammation and other pathologies, such as cancer proliferation, have led to the development of COX-2 selective inhibitors to improve the therapeutic potency and to reduce the classical side effects associated with the use of conventional NSAIDs.[5–7]

Research efforts in the discovery of COX-2 selective agents have produced many classes of compounds having desired selectivity.[8–10] A large number of compounds with common structural features, that is, the presence of two aryl rings on adjacent carbons of a cyclic/acyclic moiety, has been investigated for COX-2 inhibition. Among these compounds, rofecoxib, celecoxib, valdecoxib and etoricoxib were approved and marketed. However, rofecoxib was banned in 2004 because of cardiac toxicity. Subsequently, some of the other coxibs have been voluntarily withdrawn from the market.[11] On the other hand, some studies have suggested that rofecoxib's adverse cardiac events may not be a class effect but rather an intrinsic chemical property related to its metabolism.[12] For this reason novel scaffolds with COX-2 selective inhibitory activity needed to be found and evaluated for their anti-inflammatory effects. A number of molecules based upon a monocyclic heterocyclic template have been investigated for their COX-2 inhibitory activity.[8–10] However, the recent success of pyrazole COX-2 inhibitors has highlighted the importance of these heterocycles in medicinal chemistry.[8]

Thus our main objective is to design novel heterocyclic compounds as specific inhibitors of COX-2 in the hope that these molecules may be further explored as powerful and novel non-ulcerogenic anti-inflammatory lead-candidates. Our strategy is intended to obtain potent anti-inflammatory activity with selec-

* Corresponding author. Tel./fax: +20 502247496.
E-mail address: naglaabdalaziz2005@yahoo.com (N.I. Abdel-Aziz).

0968-0896/$ - see front matter © 2011 Elsevier Ltd. All rights reserved.
doi:10.1016/j.bmc.2011.04.027

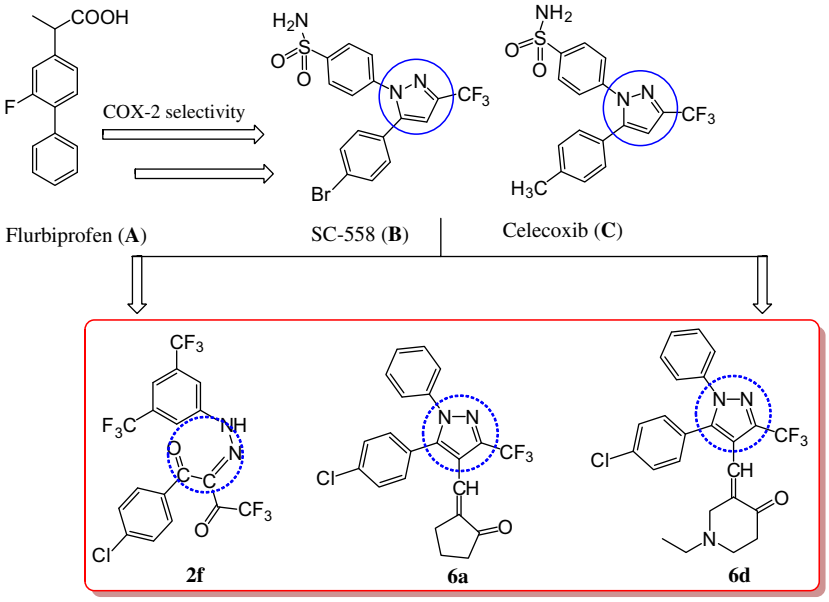

Figure 1. Representative examples of nonselective (**A**), selective (**B** and **C**) COX-2 inhibitors and the designed arylhydrazones and pyrazoles COX-2 selective inhibitors (**2**–**6**).

tive inhibition of COX-2 using traditional medicinal chemistry techniques motivated by the comparative modeling of a COX-1 and -2 complexed with flurbiprofen (**A**) and SC-558 (**B**) (Fig. 1) together with the available pharmacophore.[13,14]

In view of the previous rationale and in continuation of an ongoing program aiming at finding new structure leads with potential anti-inflammatory activities and selective COX-2 inhibition,[14,15] new series of hydrazone and pyrazole derivatives (**2**–**6**) have been synthesized and evaluated their in vitro COX-1/COX-2 inhibition, and in vivo assessment as anti-inflammatory activities (Fig. 1).

It was reported that crystal structures of COX enzymes with carboxylic acid-containing NSAIDs shows that the inhibitors are positioned in a similar fashion with their carboxylates coordinates to Arg120 and their aromatic functionality projecting into the cyclooxygenase active site towards Tyr385[13,16] and diarylheterocycles inhibitors of COX-2 bind in the cyclooxygenase active site above Arg120 and insert their sulfonamide or sulfone groups into a side pocket bordered by Val523.[17–19] Computer docking technique plays an important role in the drug design as well as in the mechanistic study by placing a molecule into the binding site of the target macromolecule in a noncovalent fashion.[20] MOE 2008.10[21] as flexible docking program enables us to predict favorable protein–ligand complex structures with reasonable accuracy and speed. The docking technique will undoubtedly continue to play an important role in drug discovery.[22] So, we docked the most active COX-2 inhibitors into COX-2 (1CX2) active site in order to predict their binding modes, their binding affinities and orientation of these compounds at the active site of the COX-2 enzyme.

2. Results and discussion

2.1. Chemistry

The designed target compounds were obtained as outlined in Schemes 1 and 2 starting with trifluoromethyl-1,3-diketone **1**.

2.1.1. Synthesis of compounds 1–3 (Scheme 1)

Claisen condensation of *p*-chloroacetophenone with ethyl trifluoroacetate provided trifluoromethyl-1,3-dicarbonyl adduct **1** in a good yield. Coupling the diazonium salt of different aromatic amines with compound **1** afforded the corresponding hydrazone derivatives **2a**–**f**. The latter compounds have the tautomeric relation with azo-hydrazo system. The structures of compounds **2** were established on the basis of their elemental analyses and spectral data. For example, the IR spectra were characterized by the presence of strong absorption bands at 3397–3345 cm^{-1}, 1683–1633 cm^{-1} and 1597–1536 cm^{-1} representing (NH), (C=O) and (–C=N–) groups, respectively. The diketone moieties in compounds **2a**–**f** were replaced with hydrazine hydrate in refluxing ethanol affording the corresponding pyrazole derivatives **3a**–**f**. The spectral and microanalytical data for compounds **3a**–**f** were consistent with their chemical structures. For example, their IR spectra were characterized by the disappearance of the absorption bands of the carbonyl groups.

2.1.2. Synthesis of compounds 4–6 (Scheme 2)

1,5-Diphenyl-3-trifluoropyrazole derivatives containing various substituents at 4-position were synthesized as outlined in Scheme 2. Cyclocondensation of phenylhydrazine with trifluoromethyl-1,3-diketone **1** afforded the corresponding 1,5-diphenylpyrazole derivatives **4** as the major product. The NH_2 in phenylhydrazine is more nucleophilic than NH and would react preferentially with the more reactive carbonyl group ($COCF_3$) leading to the production of 1,5-diphenylpyrazole regioisomer as a major product specially if the reaction is carried out in acidic medium.[23] Moreover, Vilsmeier formylation of 1,5-diphenylpyrazole derivative **4** provided the corresponding aldehyde **5** which upon treatment with different ketones afforded the respective chalcone derivatives **6**. The structures of the isolated products **4**–**6** were established on the basis of their elemental and spectral analyses.

2.2. Biological activity

2.2.1. In vivo antiinflammatory studies

All the newly synthesized compounds and diclofenac sodium, as a reference drug, were subjected to in vivo anti-inflammatory studies using the well-known rat carrageenan-induced foot paw oedema model. The results of anti-inflammatory activities against carrageenan-induced rat paw oedema and ED_{50} (mg/kg) of the

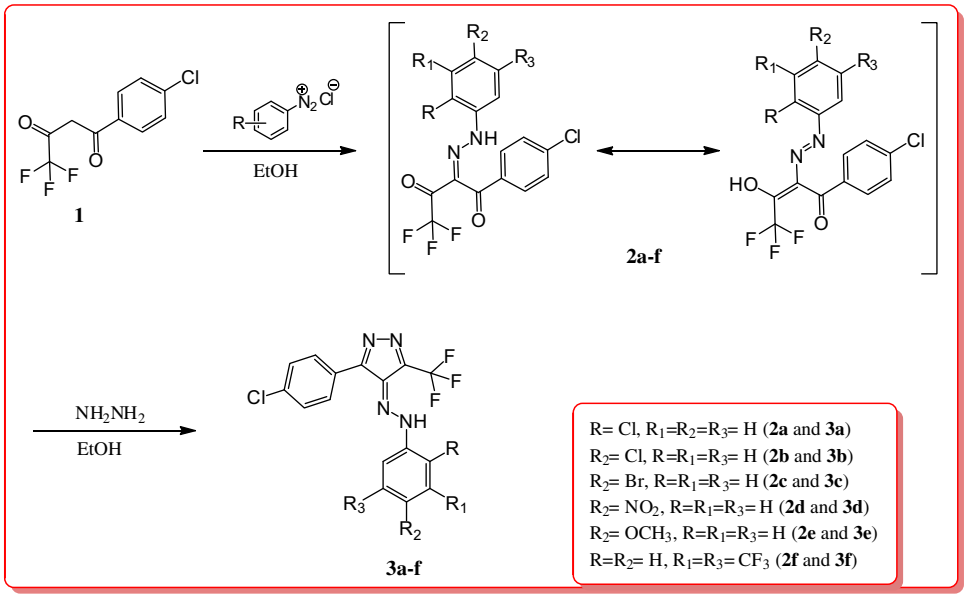

Scheme 1. Synthesis of the designed arylhydrazone and pyrazole derivatives.

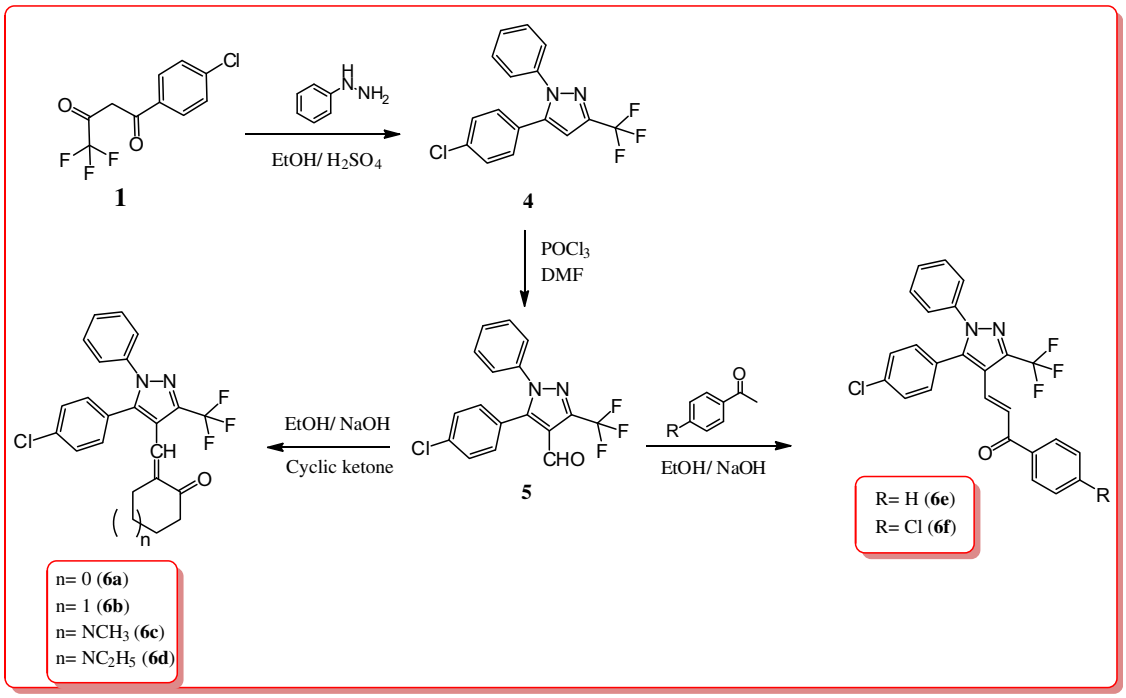

Scheme 2. Synthesis of the designed pyrazoles.

tested compounds were shown in (Table 1). All the tested compounds showed reasonable percentages of oedema reduction in the range of 4.0–89.7%. The major exception proved to be compound **3e** being inactive at the used dose. Compounds **2f**, **5**, **6a** and **6d** showed the highest anti-inflammatory activity among the tested compounds.

From the structure–activity relationship (SAR) viewpoint, the anti-inflammatory activity of the series **2a–f** and **6a–d** such as 1-(4-chlorophenyl)-2-(2-(3,5-bis(trifluoromethyl)phenyl)hydrazone)-4,4,4-trifuorobutane-1,3-dione (**2f**), 2-((5-(4-chlorophenyl)-1-phenyl-3-(trifluoromethyl)-1*H*-pyrazol-4-yl)methylene)cyclopentanone (**6a**) and 3-((5-(4-chlorophenyl)-1-phenyl-3-(trifluoromethyl)-1*H*-pyrazol-4-yl)methylene)-1-ethylpiperidin-4-one (**6d**) was found to be the highest one compared with series **3a–b**,**d–f** and **6e–f**. However, series **3a–b**,**d–f** and **6e–f** showed the least inhibitory effect (2.6–28.8%).

In series **2** arylhydrazone derivative of substituted *p*-nitrophenyl **2d** was more potent anti-inflammatory compound than chloro or methoxyphenyl derivative **2a–b** and **2e** (NO_2 > Cl and OCH_3). The anti-inflammation effect of the *p*-chlorophenyl derivative **2b** is less than that of its *o*-chlorophenyl derivative **2a**. In addition, the introduction of CF_3 moiety into the phenyl derivative of hydrazone system **2f** was found to be highly effective (88.4%) than its chlorinated one **2a–b** (35.2–41.7%). As for pyrazole series **6a–d**,

Table 1
Data of the in vivo anti-inflammatory activity of the designed compounds against carrageenan-induced rat paw oedema (IP)

Compound no.	% Inhibition of oedema[a]		ED_{50}[e]	
	After 1 h[b]	After 2 h[b]	mg/kg	mmol/kg
2a	47.1 (0.0)	41.7 (19.3)	260	0.668
2b	26.7	35.2	—	
2c	35.0 (0.0)	33.8 (13.9)	280	0.646
2d	35.8 (0.0)	57.3 (17.9)	170	0.425
2e	27.6 (0.0)	42.2 (3.8)	240	0.624
2f	80.0 (33.0)	88.4 (59.0)	112	0.228
3a	38.4	15.1	—	
3b	8.1	9.1	—	
3c	26.3 (17.5)	52.1 (31.3)	180	0.419
3d	4.0	7.0	—	
3e	NA[c]	NA[c]	—	
3f	40.8 (3.4)	28.8 (17.3)	—	
5	75.0 (24.1)	59.1 (40.3)	190	0.542
6a	80.7 (37.0)	82.0 (67.0)	118	0.274
6b	33.7	23.9	—	
6c	6.7	20.3	—	
6d	80.0 (41.0)	89.7 (64.0)	120	0.261
6e	1.8	2.6	—	
6f	1.5	4.4	—	
Diclofenac[d]	88.5	89.5	114	0.358

[a] The results are expressed as means ± SEM (n = 4–6) following a 200 mg/kg IP of the test compound.
[b] Values in parenthesis are determined at 100 mg/kg IP.
[c] No activity was observed at the used dose.
[d] Values are determined at 100 mg/kg IP.
[e] ED_{50} was the effective dose calculated after 2 h.

Table 2
Data of the in vitro COX-1/COX-2 enzyme inhibition assay of the designed compounds

Compound no.	IC_{50}(μM)[a]		SI[d]
	COX-1[b]	COX-2	
2a	>50[c]	0.90	54.9
2b	>50	0.91	54.9
2c	>50	0.91	54.9
2d	>50[c]	0.90	54.9
2e	>50[c]	2.95	16.9
2f	>50	0.45	111.1
3a	>50	45	1.1
3b	>50	40	1.3
3c	>50	3.00	16.7
3d	>50	45	1.1
3e	>50	45	1.1
3f	>50	45	1.1
5	>50	0.55	90.9
6a	>50	0.45	111.1
6b	>50	45	1.1
6c	>50	10	5.0
6d	>50	0.45	111.1
6e	>50	45	1.1
6f	>50	45	1.1
Diclofenac	0.16	2.5	0.06
Celecoxib	>50	0.30	166.7

[a] IC_{50} value is the compound concentration required to produce 50% inhibition of COX-1 or COX-2 for means of two determinations and deviation from the mean is <10% of the mean value.
[b] No inhibition of COX-1 up to 50 μM and precipitation of compounds observed beyond this concentration.
[c] Compounds **2a**, **2d** and **2e** showed 31% inhibition of COX-1 at 0.5 μM and only 25% inhibition of COX-1 at 100 μM.
[d] Selectivity index (COX-1 IC_{50}/COX-2 IC_{50}).

compounds **6a** and **6d** showed very good activity (82.0% and 89.7% reduction, respectively) more than **6b** and **6c** (23.9% and 20.3% reduction, respectively), while compound **6e** and **6f** had slight activity (2.6% and 4.4% reduction, respectively). These results revealed the importance of the cycloalkane moiety for the anti-inflammatory activity of series **6**.

It should be noted that administration of compounds **3a**, **3f** and **5** produced maximum inhibition of inflammation one hour after administration of carrageenan. At 2 h after carrageenan the percentage inhibition of inflammation was greatly reduced as it was clearly observed with compound **5** which showed high anti-inflammatory activity 1 h after carrageenan. This finding could be explained by a rapid metabolism of this compound.

ED_{50} of the compounds, which were shown promising degree of anti-inflammatory activity (33.8–89.7%), were studied. Compounds **2d**, **3c**, **5**, **6a** and **6d** exhibited better anti-inflammatory activity with ED_{50} of 170, 180, 190, 118 and 120 mg/kg, respectively, as compared to diclofenac (ED_{50} = 114 mg/kg). In the carrageenan-induced rat paw oedema assay model, compound **2f** was the most potent anti-inflammatory agent (ED_{50} = 112 mg/kg) within this group of compounds at 2 h postdrug administration.

2.2.2. In vitro cyclooxygenase (COX) inhibition assay

The second target of the biological activity tests was the study of the ability of the tested compounds to inhibit ovine COX-1 and COX-2 using an enzyme immunoassay (EIA) kit. The efficacies of the tested compounds were determined as the concentration causing 50% enzyme inhibition (IC_{50}) (Table 2). As far as COX-1 inhibitory properties are concerned, all the tested compounds showed no inhibition of COX-1 up to 50 μM. Moreover, a reasonable in vitro COX-2 inhibitory activity was observed with compounds **2f**, **6a**, **6d** with IC_{50} 0.45 μM and for compound **5** with IC_{50} 0.55 μM. The selectivity indices (COX-1/COX-2) were calculated and compared with that of the standard COX-2 selective inhibitor, celecoxib.

In the assay system, the IC_{50} values of celecoxib on COX-1 and COX-2 were determined to be >50 and 0.30 μM, indicating that celecoxb is a selective COX-2 inhibitor. The results showed that most of the compounds showed potent inhibition against COX-2 ($IC_{50} \cong 0.45–10.0$ μM) compared to the inhibition for COX-1 (IC_{50} >50 μM) as listed in (Table 2). Nearly 4 of the compounds (**2f**, **5**, **6a** and **6d**) were found to be potent and selective similar to celecoxib against COX-2. The effects of substituents introduced into the hydrazones and pyrazoles **2**–**6** were revealed to be directional, being dependent on the electronic nature of the substituents and the ring size of the cycloalkanone fragments, that is, introduction of electron-withdrawal group at the phenyl group of hydrazones **2a**–**d** enhanced COX-2-inhibiting activity with a COX-2-selectivity (SI = 54.9). Moreover introduction of electron-donating such as methoxy as for compound **2e** resulted in lowering the COX-2-inhibiting activity (SI = 16.9), while introduction of a CF_3 group as compound **2f** showed just the opposite effects, resulting in a COX-2-selective inhibitor (SI = 111.1). The activities of pyrazole derivatives **5**–**6** are shown in Table 2. Among them, compounds **5**, **6a** and **6d** are COX-2-selective inhibitors (SI = 90.9–111.1). Interestingly the size of cycloalkanone fragment on the pyrazole core plays critical roles in the COX-inhibiting activity of the tested compounds. The cyclopentanone analogue **6a** showed the most potent activity, being 100 times more active than cyclohexanone analogue **6b** COX-2- inhibiting activity and has similar activity to *N*-ethylpiperidone analogue **6d**. This result, as well as the previously described effect of the substitution on phenyl suggests the importance of electronic effects on hydrazone derivatives and spatial structure around the pyrazole core.

2.3. Molecular docking results

Insights into the differences between the binding sites of COX-1and COX-2 obtained from X-ray crystal structure data,[13,24] provided useful guidelines that facilitated the design of the selective COX-2 inhibitors. For example, the COX-2 binding site possesses an additional 2°-pocket, that is, absent in COX-1, which is highly

relevant to the design of selective COX-2 inhibitors. This COX-2 2°-pocket arises due to a conformational change at Tyr355, that is, attributed to the presence of Ile523 in COX-1 relative to Val523 having a smaller side chain in COX-2.[24] It has also been reported that replacement of His513 in COX-1 by Arg513 in COX-2 plays a key role with respect to the H-bond network in the COX-2 binding site. Access of ligands to the 2°-pocket of COX-2 is controlled by histidine (His90), glutamine (Gln192), and tyrosine (Tyr355).[25] Interaction of Arg513 with the bound drug is a requirement for time dependent inhibition of COX-2.[26]

The level of COX-2 inhibition and anti-inflammatory activities of compounds **2f**, **6a** and **6d** prompted us to perform molecular docking studies to understand the ligand–protein interactions in detail. All the calculations were performed using MOE 2008.10 software installed on 2.0G Core 2 Duo.[21,27] The crystal structures of COX-2 enzymes complexed with SC-558 [1CX2] were used for the docking.[13] The active site of the enzyme was defined to include residues within a 10.0 Å radius to any of the inhibitor atoms. The automated docking program of MOE 2008.10 was used to dock compounds **2f**, **6a** and **6d** on the active sites of COX-2 enzymes. The most stable docking model was selected according to the best scored conformation predicted by the MOE scoring function. The complexes were energy-minimized with a MMFF94 force field[28] till the gradient convergence 0.05 kcal/mol was reached. To compare orientations of the ligands, we superimposed each compound's best pose which as obtained by regarding the S score in MOE. With few exceptions, all the ligands showed similar orientation in the COX-2 active site and the complex formed was stabilized by formation of classical and non-classical hydrogen bonds (Fig. 2).[29,30] In general, it is observed that the *p*-chlorophenyl fragment of the compounds fitted into the cavity formed by Leu531, Tyr385, Trp387, Ala527 and Val349 while the other phenyl moiety fitted into the other cavity formed by Phe518, Leu352, Ser353, Tyr355, Val523 and Arg120. As Kurumbail et al.[13] mentioned, these features are common in non-selective and selective COX-2 inhibitors such as flurbiprofen and SC-558. On the other hand, it is known that the main difference between the two COX active sites is the replacement of Ile523 in COX-1 by Val523, a less bulky amino acid. This replacement creates an adjunct pocket in the COX-2 active site which may be responsible for selectivity. Our docking study showed that compounds **2f**, **6a** and **6d** were oriented so that their 3,5-ditrifluoromethylphenyl fragment (**2f**) and phenyl moiety (**6a**, **6d**) fill this adjunct pocket. This may explain why the compounds show significant selective activity against COX-2 enzyme. Compound **2f** produces a deep moving into the hydrophilic pocket of COX-2 with which the 3,5-ditrifluoromethylphenyl and hydrazone fragments are able to reach the hydrophilic pocket and is involved in strong hydrogen bonding with His90 (NH–F; 2.91 Å), Arg120 (NH–C=O; 2.95 Å) and Tyr355 (OH–NH; 2.91 Å) and weak hydrogen bonding with Tyr355 (OH–NH; 3.23 Å, OH–C=O; 3.47 Å). Such interactions are almost essential for COX-2 inhibitory activity, as exemplified by the binding interaction of SC-558, an analogue of

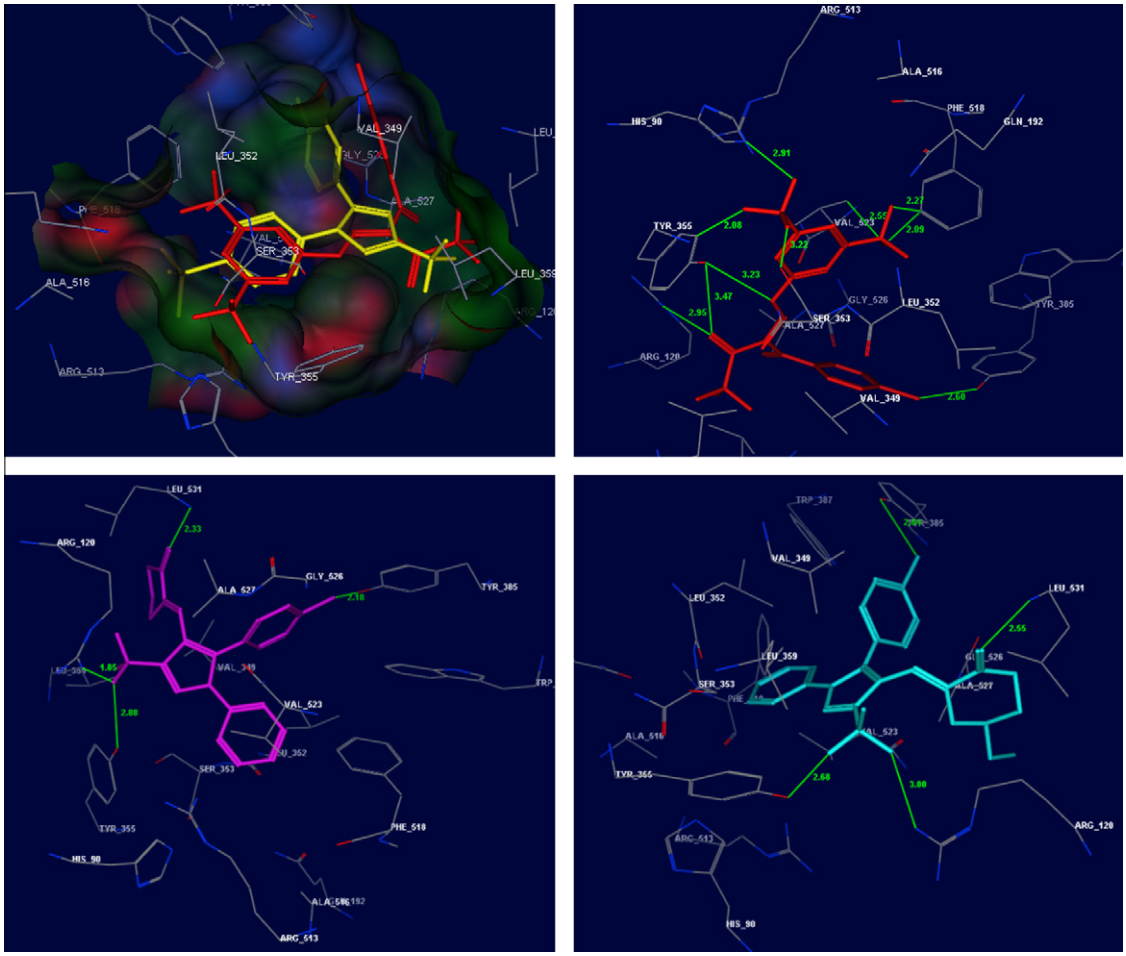

Figure 2. The orientation of **2f** (color red) in COX-2 active pocket (upper left panel; SC-558 is shown as yellow). The orientation of **2f** (upper right panel; color red), **6a** (lower left panel; color violet) and **6d** (lower right panel; color cyan) in COX-2 active pocket (H bonds are shown as green).

celecoxib cocrystallized in the COX-2 active site.[13] Additionally this complex of compound **2f** was shown nonclassical hydrogen bonds of type CH–F among Val523, Phe518 and **2f**. In addition; such interaction forces the *p*-clorophenyl fragment to adopt a specific orientation to be involved in hydrophobic interaction with Trp387, Tyr385, Val349 and Leu531. The lateral pocket of COX-2 would therefore be responsible for the COX-2 selectivity of **2f** and contributed to stabilize the ligand–enzyme complexes (Fig. 2).

The complex generated by docking studies of **2f** with COX-2 and superimposition with the structure of the selective inhibitor, SC-558, co-crystallized with COX-2, illustrated in Figure 2, shows that compound **2f** can bind in the active site of this enzyme in approximately similar fashion as the pyrazolic prototype (SC-558). Comparison of the interactions performed by SC-558 in the crystal and the docked structure of **2f** with COX-2 (Fig. 2) shows that the trifluorophenyl groups of **2f** hydrogen bonded to the amino acid residue His90, similarly to the sulfonyl moiety of the pharmacophoric sulfonamide group pertaining to SC-558. Moreover, an additional hydrogen bond was observed between the carbonyl oxygen and Arg120 and Tyr355. Additionally, 3,5-ditrifluoromethylphenyl system are positioned in the same region as *p*-sulfonamido-phenyl ring of SC-558, while, the *p*-chlorophenyl of compound **2f** is close to the *p*-Br-phenyl ring of SC-558, in the aromatic region of the active site lined by aromatic amino acid residues such as Tyr385 and Trp387, among others. In short, the described interactions are typical of selective inhibitors of COX-2, confirming the molecular design of the reported class of anti-inflammatory hydrazone and pyrazole derivatives.[8–10] Similarly, compounds **6a** and **6d** can bind in the active site of this enzyme in approximately similar fashion SC-558 with an additional non-classical hydrogen bond as described above.

On the other hand, compounds **2f** and **6a** as representative examples were modeled into the active site of COX-1 enzyme to understand the inactivity of such compounds toward COX-1 inhibition (Table 3, Fig. 3). The crystal structures of COX-1 enzymes complexed with flurbiprofen[31] [1EQH] were used for the docking using the same protocol described above. The two compounds could dock into the active site of COX-1 successfully. The insufficient binding of both compounds can be explained in terms of the occurrence of very weak hydrogen bonds in which the benzoyl carbonyl group of compound **2f** formed such weak bonds with Arg120 (3.7 Å) and Tyr355 (3.3 Å) while CF_3 group of compound **6a** formed similar weak bonds with Ala527 (3.14 Å) and Gly526 (3.42 Å).

Table 3
Docking results of compounds **2f**, **6a** and **6d** into the active sites of COX-1 and COX-2

Compound no.	Against COX-1[a]		Against COX-2[a]	
	No. H-bond[b] (strength)[c]	$E_{int.}$ (kcal mol^{-1})[d]	No. H-bond[b] (strength)[c]	$E_{int.}$ (kcal mol^{-1}) [d]
2f	2 (weak)	−9.6	7 (strong) 3 (weak)	−61.41
6a	2 (weak)	−6.7	4 (strong)	−51.06
6d	—	—	4 (strong)	−53.88

[a] Details of hydrogen bonding are explained in Figures 2 and 3.
[b] Hydrogen bondings are refered to classical and nonclassical hydrogen bonds.
[c] Strength of hydrogen bond refered to the length of such hydrogen bond (>3.0 Å = weak and <3.0 Å = strong).
[d] Interaction energy between the ligand and receptor.

3. Conclusion

The present study describes the synthesis of new arylhydrazone derivatives and a series of 1,5-diphenyl pyrazoles. The biological tests showed that the new compounds with anti-inflammatory activities were less active than diclofenac against COX-1. However, compounds **2f**, **5**, **6a** and **6d** showed reasonable inhibitory profiles against COX-2, indicating that they are selective inhibitors for COX-2. Moreover, the study showed that compounds **2f**, **5**, **6a** and **6d** were the most selective among the tested compounds with selectivity index in the range of 90.9–111.1. The binding mode of the tested compounds inside the COX-2 active site was predicted using a docking technique. When the results of the inhibitory activity and docking studies are considered together, it can be suggested that: (i) the arylhydrazone moiety, which fill the adjunct pocket in the COX-2 active site, make contribution to the selectivity; is a suitable scaffold for COX-2 enzyme; (ii) pyrazoles with appropriate substitutions which can fill the adjunct pocket and interact with the relatively polar residues such as Gln192 and Arg513 may be useful to propose new molecules with enhanced selectivity towards COX-2.

4. Experimental

4.1. Chemistry

Melting points was determined using *Fisher–Johns* melting point apparatus and are uncorrected. Infrared (IR) spectra were recorded on Mattson 5000 FT-IR spectrometer. NMR spectra were

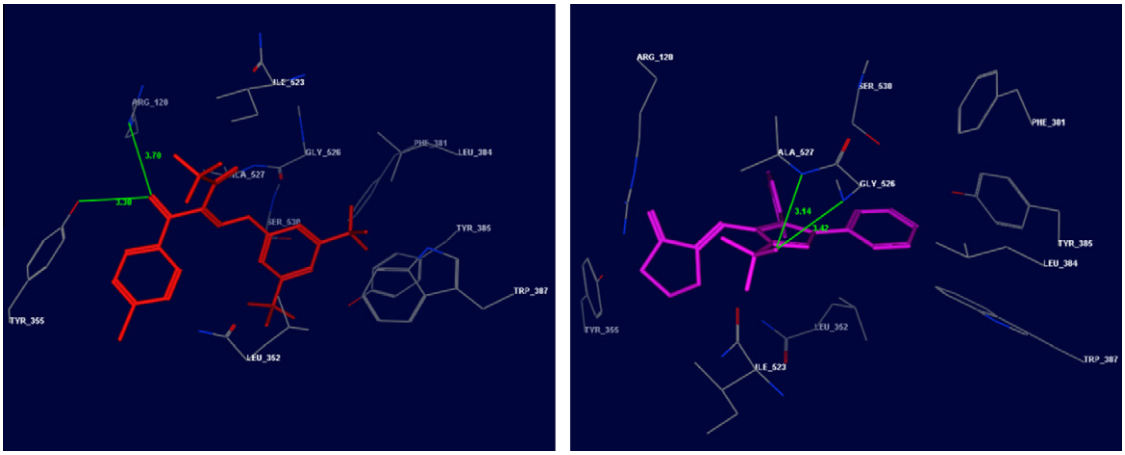

Figure 3. The orientation of **2f** (left panel; color red) and **6a** (right panel; color violet) in COX-1 active pocket (H bonds are shown as green).

recorded on FT-NMR spectrometer (200 MHz) Gemini Varian using DMSO-d_6 and on Ultra shield Bruker (500 MHz) using $CDCl_3$ and TMS was used as internal standard. Mass spectra were measured on JEOL JMS-600H spectrometer. Elemental analysis was carried out for C, H and N at the Microanalytical Center of Cairo University. All reagents were purchased from the Aldrich Chemical Company. The well-known compounds, 1-(4-chlorophenyl)-4,4,4-trifuorobutane-1,3-dione **1**[23] and **4**[32,33] were prepared following the procedures reported in the literature.

4.1.1. General method for synthesis of 1-(4-chlorophenyl)-2-(2-arylhydrazone)-4,4,4-trifuorobutane-1,3-dione (2a–f) (Scheme 1)

A cooled sodium nitrite solution (1.5 g in 10 mL of water) was added dropwise during 10 min to an ice-cold solution of the appropriate aniline in concentrated hydrochloric acid (3 mL). The reaction mixture was stirred for 30 min at the same temperature and for 2 h at room temperature to give the corresponding diazonium salt. The solution of diazonium salt was added dropwise with stirring to an ice-cold mixture of trifluoromethyl-1,3-diketone **1** (2.5 g, 0.01 mol) in sodium acetate (4.19 g, 0.05 mol) and ethanol (50 mL) over 15 min. The stirring was continued for 30 min and the solid obtained was collected and crystallized from ethanol to give the corresponding hydrazones **2a**–**f**.

4.1.1.1. 1-(4-Chlorophenyl)-2-(2-(2-chlorophenyl)hydrazone)-4,4,4-trifuorobutane-1,3-dione (2a). Yield, 90%; mp 55–56 °C; IR (KBr) ν_{max}/cm^{-1} 3278 (NH), 1675, 1635 (C=O), 1596, 1536 (C=N). ^1H NMR ($CDCl_3$): δ 14.15 (s, 1H, NH), 7.78 (d, 1H, J = 8.0 Hz), 7.48 (d, 2H, J = 8.5 Hz), 7.40–7.34 (4H, m), 7.15–7.12 (m, 1H). ^{13}C NMR ($CDCl_3$): δ 117.3, 122.9, 127.4, 128.5, 128.7, 129.8, 129.9, 131.9, 135.7, 137.2, 138.6, 139.6, 177.1, 190.5. MS *m/z* (%); 388.00 (58.99, M^+), 111.00 (60.67), 75.00 (65.17), 63.00 (76.97), 50.00 (100.00). Anal. Calcd for $C_{16}H_9Cl_2F_3N_2O_2$ (%): C, 49.38; H, 2.33; N, 7.20. Found: C, 49.02; H, 2.51; N, 7.80.

4.1.1.2. 1-(4-Chlorophenyl)-2-(2-(4-chlorophenyl)hydrazone)-4,4,4-trifuorobutane-1,3-dione (2b). Yield, 85%; mp 59–62 °C; IR (KBr) ν_{max}/cm^{-1} 3245 (NH), 1673, 1640 (C=O), 1590, 1540 (C=N). ^1H NMR (DMSO-d_6); δ 11.90 (s, 1H, NH), 8.10–7.20 (m, 8H, Ar-H). Anal. Calcd for $C_{16}H_9Cl_2F_3N_2O_2$ (%): C, 49.38; H,2.33; N, 7.20. Found: C, 49.70; H, 2.00; N,7.70.

4.1.1.3. 1-(4-Chlorophenyl)-2-(2-(4-bromophenyl)hydrazone)-4,4,4-trifuorobutane-1,3-dione(2c). Yield, 85%; mp 90–92 °C; IR (KBr) ν_{max}/cm^{-1} 3340 (NH), 1680, 1665 (C=O), 1592, 1545 (C=N). ^1H NMR (DMSO-d_6); δ 11.60 (s, 1H, NH), 7.91–7.40(m, 8H, Ar-H). Anal. Calcd for $C_{16}H_9BrClF_3N_2O_2$ (%): C, 44.32; H, 2.09; N, 6.46. Found: C, 44.80; H,1.80; N, 6.91.

4.1.1.4. 1-(4-Chlorophenyl)-2-(2-(4-nitrophenyl)hydrazone)-4,4,4-trifuorobutane-1,3-dione (2d). Yield, 80%; mp 109–110 °C; IR (KBr) ν_{max}/cm^{-1} 3250 (NH), 1660, 1650 (C=O), 1580, 1570 (C=N). ^1H NMR (DMSO-d_6); δ 11.95 (s, 1H, NH), 8.21–7.40(m, 8H, Ar-H). MS *m/z* (%); 401.00 (33.10, M^++2) 399.90 (28.78, M^++1), 399.00 (100.00, M^+), 262.85 (27.06), 249.00 (0.78), 113.00 (10.90). Anal. Calcd for $C_{16}H_9ClF_3N_3O_4$ (%): C, 48.08; H, 2.27; N, 10.51. Found: C, 47.80; H, 1.91; N, 11.00.

4.1.1.5. 1-(4-Chlorophenyl)-2-(2-(4-methoxyphenyl)hydrazone)-4,4,4-trifuorobutane-1,3-dione (2e). Yield, 75%; mp 50–52 °C; IR (KBr) ν_{max}/cm^{-1} 3397 (NH), 1677, 1633 (C=O), 1594, 1536 (C=N). ^1H NMR ($CDCl_3$): δ 14.40 (s, 1H, NH), 7.45 (d, 2H, J = 8.5 Hz), 7.39 (d, 2H, J = 8.0 Hz), 7.34 (d, 2H, J = 8.5 Hz), 6.92 (d, 2H, J = 9.0 Hz), 3.78 (s, 3H, OCH_3). ^{13}C NMR ($CDCl_3$): δ 55.6, 115.2, 118.7, 127.2, 128.4, 128.5, 129.7, 131.8, 134.0, 136.3, 139.0, 159.3, 176.7, 191.2. Anal. Calcd for $C_{17}H_{12}ClF_3N_2O_3$ (%): C, 53.07; H, 3.14; N, 7.28. Found: C, 53.40; H, 3.40; N, 7.65.

4.1.1.6. 1-(4-Chlorophenyl)-2-(2-(3,5-bis(trifluoromethyl)phenyl)hydrazone)-4,4,4-trifuorobutane-1,3-dione (2f). Yield, 95%; mp 44–46 °C; IR (KBr) ν_{max}/cm^{-1} 3350 (NH), 1683, 1670 (C=O), 1597,1537 (C=N). ^1H NMR ($CDCl_3$): δ 14.7 (s, 1H, NH), 7.94–7.36 (m,7H, Ar-H). ^{13}C NMR ($CDCl_3$): δ 115.9, 117.6, 122.9, 124.7, 126.3, 126.6, 126.9, 128.7, 129.2, 131.8, 133.8, 135.5, 138.3, 139.8, 177.1, 190.5. MS *m/z* (%); 490.00 (0.15, M^+), 423.95 (0.81), 421.95 (2.46), 222.90 (0.30), 220.95 (0.89),139.00 (100.00),. Anal. Calcd for $C_{18}H_8ClF_9N_2O_2$ (%): C, 44.06; H, 1.64; N, 5.71. Found: C, 44.41; H, 2.00; N, 6.02.

4.1.2. General method for synthesis of 3-(4-chlorophenyl)-4-(2-arylhydrazono)-5-trifuoromethyl)-4*H*-pyrazoles ((3a–f) (Scheme 1)

A mixture of the appropriate hydrazone **2a**–**f** (0.01 mol) and hydrazine hydrate (0.03 mol) was refluxed in ethanol (20 mL) for 4 h. The reaction mixture was allowed to cool, diluted with water and the solid obtained was crystallized from ethanol to give **3a**–**f**.

4.1.2.1. 3-(4-Chlorophenyl)-4-(2-(2-chlorophenyl)hydrazono)-5-trifuoromethyl)-4*H*-pyrazole (3a). Yield, 65%; mp 109–110 °C; IR (KBr) ν_{max}/cm^{-1} 3297 (NH), 1599, 1547 (C=N). ^1H NMR ($CDCl_3$): δ 11.55 (s, 1H, NH), 7.40–7.14 (m, 8H, Ar-H). ^{13}C NMR ($CDCl_3$): δ 118.6, 120.7, 122.8, 124.8, 126.1, 126.9, 127.4, 128.3, 128.5, 129.6, 130.4, 131.1, 134.4. Anal. Calcd for $C_{16}H_9Cl_2F_3N_4$ (%): C, 49.89; H, 2.36; N, 14.55. Found: C, 50.10; H, 2.70; N, 15.00.

4.1.2.2. 3-(4-Chlorophenyl)-4-(2-(4-chlorophenyl)hydrazono)-5-trifuoromethyl)-4*H*-pyrazole (3b). Yield, 55%; mp 124–126 °C; ^1H NMR ($CDCl_3$): δ 7.44–7.36 (m, 8H, Ar-H), 7.34 (s, 1H, NH). ^{13}C NMR ($CDCl_3$): δ 120.7, 122.8, 124.9, 126.9, 127.4, 129.6, 130.3, 130.8, 131.1, 134.5. MS *m/z* (%); 386.20 (26.47, M^+), 265.20 (41.42), 250.20 (1.47), 147.10 (75.98), 95.05 (100.00). Anal. Calcd for $C_{16}H_9Cl_2F_3N_4$ (%): C, 49.89; H, 2.36; N, 14.55. Found: C, 50.11; H, 2.40; N, 15.00.

4.1.2.3. 3-(4-Chlorophenyl)-4-(2-(4-bromophenyl)hydrazono)-5-trifuoromethyl)-4*H*-pyrazole (3c). Yield, 45%; mp 110–111 °C; ^1H NMR ($CDCl_3$): δ 11.99 (s, 1H, NH), 7.49–6.65 (m, 8H, Ar-H). ^{13}C NMR ($CDCl_3$): δ 101.4, 119.8, 121.9, 126.4, 126.9, 127.4, 129.5, 131.3, 135.5, 144.3. MS *m/z* (%); 430.00 (61.45, M^+), 363.00 (68.07), 108.00 (63.25), 69.00 (100.00), 50.00 (82.53). Anal. Calcd for $C_{16}H_9BrClF_3N_4$ (%): C, 44.73; H, 2.11; N, 13.04. Found: C, 45.00; H, 2.14; N, 13.50.

4.1.2.4. 3-(4-Chlorophenyl)-4-(2-(4-nitrophenyl)hydrazono)-5-trifuoromethyl)-4*H*-pyrazole (*3d*). Yield, 55%; mp 105–107 °C; IR (KBr) ν_{max}/cm^{-1} 3311 (NH), 1597,1545 (C=N). ^1H NMR (DMSO-d_6); δ 13.00 (s, 1H, NH), 8.00–7.20 (m, 8H, Ar-H). MS *m/z* (%); 395.10 (41.43, M^+), 259.90 (43.59), 152.25 (4.99), 150.20 (27.94), 110.00 (100.00). Anal. Calcd for $C_{16}H_9ClF_3N_5O_2$ (%): C, 48.56; H, 2.29; N, 17.70. Found: C, 48.66; H, 2.50; N, 17.15.

4.1.2.5. 3-(4-Chlorophenyl)-4-(2-(4-methoxyphenyl)hydrazono)-5-trifuoromethyl)-4*H*-pyrazole (3e). Yield, 40%; mp 98–100 °C; ^1H NMR ($CDCl_3$): δ 12.55 (s, 1H, NH), 7.37–6.59 (m, 8H, Ar-H), 3.26 (s, 3H, OCH_3). ^{13}C NMR ($CDCl_3$): δ 56.1, 101.2, 119.8, 120.7, 122.0, 122.8, 126.4, 126.8, 127.3, 129.4, 129.5, 130.5, 134.4, 135.4, 14.4. MS *m/z* (%); 382.05 (13.11, M^++2), 380.00 (40.76, M^+), 350.20 (46.44), 127.50 (18.26), 125.40 (51.91), 108.05 (100.00). Anal. Calcd for $C_{17}H_{12}ClF_3N_4O$ (%): C, 53.63; H, 3.18; N, 14.71. Found: C, 53.90; H, 2.91; N, 15.00.

4.1.2.6. 3-(4-Chlorophenyl)-4-(2-(3,5-bis(trifluoromethyl)phenyl)hydrazono)-5-trifuoromethyl)-4*H*-pyrazole (3f). Yield, 60%; mp 122–123 °C; ^{1}H NMR (DMSO-d_6); δ 13.50 (s, 1H, NH), 7.84–7.26 (m, 7H, Ar-H). Anal. Calcd for $C_{18}H_8ClF_9N_4$ (%): C, 44.42; H, 1.66; N, 11.51. Found: C, 44.00; H, 2.00; N, 12.00.

4.1.3. Method for synthesis of 5-(4-chlorophenyl)-1-phenyl-3-(trifluoromethyl)-1*H*-pyrazole-4-carbaldehyde (5) (Scheme 2)

A solution of compound **4** (16.13 g, 0.05 mole) in dimethyl formamide (26 mL) was heated at 90 °C, phosphorous oxychloride (10 mL, 0.06 mole) was added dropwise with stirring and the stirring was continued for 7 h. A solution of phosphorous oxychloride (10 mL, 0.06 mole) in dimethyl formamide (26 mL) were added to the reaction mixture at room temperature and the reaction mixture was heated at 90 °C for 2 h. The reaction mixture was allowed to cooled to 0 °C by cautious addition of ice water and neutralized with sodium hydroxide (130 mL, 2 N). The reaction mixture was extracted with ethyl acetate, the organic layer was washed with water, brine, dried over anhydrous sodium sulphate, the solvent was evaporated under reduced pressure and the residue was crystallized from chloroform; yield, 40%; mp 55–58 °C; ^{1}H NMR ($CDCl_3$): δ 9.96 (s, 1H, CHO), 8.46 (s, 1H), 7.76 (d, 2H, J = 8.5 Hz), 7.71 (d, 2H, J = 8.0 Hz), 7.46–7.32 (m, 4H). ^{13}C NMR ($CDCl_3$): δ 119.7, 122.5, 128.1, 128.9, 129.7, 129.8, 130.2, 123.0, 135.4, 138.9, 135.2, 184.4. Anal. Calcd for $C_{17}H_{10}ClF_3N_2O$ (%): C, 58.22; H, 2.87; N, 7.99. Found: C, 58.40; H, 3.00; N, 8.21.

4.1.4. General method for synthesis of 2 and/or 3-((5-(4-chlorophenyl)-1-phenyl-3-(trifluoromethyl)-1*H*-pyrazol-4-yl)methylene) derivatives (6a–d) (Scheme 2)

A solution of sodium hydroxide (1.20 g, 0.03 mol) in ethanol/water (34/46 mL) was added dropwise to a stirred solution of compound **5** (24.55 g, 0.07 mol) and the appropriate cyclic alkanone (1.1 mol) in ethanol (50 mL). The reaction mixture was stirred at room temperature for 6 h, the solvent was evaporated under reduced pressure and the residue was crystallized from 2-propanol.

4.1.4.1. 2-((5-(4-Chlorophenyl)-1-phenyl-3-(trifluoromethyl)-1*H*-pyrazol-4-yl)methylene) cyclopentanone (6a). Yield, 75%; mp 189–190 °C; ^{1}H NMR (DMSO-d_6); δ 8.20–7.20 (m, 10H, CH=C, Ar-H), 3.00–2.80 (m, 4H, $2CH_2$), 2.20–2.00 (m, 2H, CH_2),. Anal. Calcd for $C_{22}H_{16}ClF_3N_2O$ (%): C, 63.39; H, 3.87; N, 6.72. Found: C, 63.80; H, 4.01; N, 7.00.

4.1.4.2. 2-((5-(4-Chlorophenyl)-1-phenyl-3-(trifluoromethyl)-1*H*-pyrazol-4-yl)methylene) cyclohexanone (6b). Yield, 50%; mp 183–185 °C; ^{1}H NMR (DMSO-d_6); δ 8.20–7.20 (m, 10H, CH=C, Ar-H), 2.90–2.80 (m, 4H, $2CH_2$), 1.81–1.75 (m, 4H, $2CH_2$),. Anal. Calcd for $C_{23}H_{18}ClF_3N_2O$ (%): C, 64.12; H, 4.21; N, 6.50. Found: C, 64.50; H, 4.30; N, 6.10.

4.1.4.3. 3-((5-(4-Chlorophenyl)-1-phenyl-3-(trifluoromethyl)-1*H*-pyrazol-4-yl)methylene)-1-methyl piperidin-4-one (6c). Yield, 70%; mp 200–201 °C; ^{1}H NMR (DMSO-d_6); δ 8.11–7.40 (m, 10H, CH=C, Ar-H), 3.30 (s, 2H,CH_2), 3.10–2.70 (m, 7H, $2CH_2$, NCH_3). MS m/z (%); 445.30 (47.16, M^+), 255.40 (39.05), 125.45 (15.85), 113.05 (0.37), 82.05 (100.00). Anal. Calcd for $C_{23}H_{19}ClF_3N_3O$ (%): C, 61.96; H, 4.30; N, 9.42. Found: C, 62.05; H, 4.51; N, 10.00.

4.1.4.4. 3-((5-(4-Chlorophenyl)-1-phenyl-3-(trifluoromethyl)-1*H*-pyrazol-4-yl)methylene)-1-ethyl piperidin-4-one (6d). Yield, 45%; mp 210–212 °C; ^{1}H NMR (DMSO-d_6); δ 8.70–7.40 (m, 10H, CH=C, Ar-H), 3.80 (s, 2H, CH_2), 2.85–2.62 (q, 2H, CH_2CH_3), 2.60–2.40 (m, 4H, $2CH_2$), 1.25–1.00 (t, 3H, CH_2CH_3),. MS m/z (%); 460.30 (0.24, M^++1), 459.30 (0.39, M^+), 458.30 (0.54), 322.20 (0.71), 320.20 (2.20), 58.10 (100.00). Anal. Calcd for $C_{24}H_{21}ClF_3N_3O$ (%): C, 62.68; H, 4.60; N, 9.14. Found: C, 62.77; H, 4.80; N, 9.15.

4.1.5. General method for synthesis of 3-(5-(4-(chloro)phenyl)-1-phenyl-3-(trifluoromethyl)-1*H*-pyrazol-4-yl)-1-phenylprop-2-en-1-one derivatives 6e,f (Scheme 2)

A solution of sodium hydroxide (1.2 g, 0.03 mol) in ethanol/water (34/46 mL) was added dropwise to a stirred solution of compound **5** (24.55 g, 0.07 mol) and the appropriate ketone (1.1 mol) in ethanol (50 mL). The reaction mixture was stirred at room temperature for 6 h, the solvent was evaporated under reduced pressure and the residue was crystallized from 2-propanol.

4.1.5.1. 3-(5-(4-Chlorophenyl)-1-phenyl-3-(trifluoromethyl)-1*H*-pyrazol-4-yl)-1-phenylprop-2-en-1-one (6e). Yield, 40%; mp 186–188 °C; ^{1}H NMR ($CDCl_3$): 8.26 (s, 1H), 7.88 (d, 2H, J = 7.0 Hz), 7.77–7.74 (m, 1H), 7.70 (d, 2H, J = 8.0 Hz), 7.56 (d, 2H, J = 8.5 Hz), 7.51–7.47 (m, 1H), 7.42–7.32 (m, 6H), 7.30–7.27 (m, 1H). ^{13}C NMR ($CDCl_3$): δ 117.2, 118.3, 120.7, 125.8, 126.3, 127.0, 127.3, 127.6, 128.0, 128.6, 129.1, 129.8, 131.7, 133.8, 137.0, 138.3, 151.5, 183.3, 188.9. MS m/z (%); 452.35 (45.85, M^+), 132.16 (41.35), 120.15 (12.18), 106.12 (64.87), 49.65 (100.00). Anal. Calcd for $C_{25}H_{16}ClF_3N_2O$ (%): C, 66.31; H; 3.56; N, 6.19. Found: C, 66.45; H, 3.20; N, 6.60.

4.1.5.2. 1-(4-Chlorophenyl)-3-(5-(4-chlorophenyl)-1-phenyl-3-(trifluoromethyl)-1*H*-pyrazol-4-yl))prop-2-en-1-one (6f). Yield, 40%; mp 173–175 °C; ^{1}H NMR (DMSO-d_6); δ 7.81–7.40 (m, 15H, CH=CH, Ar-H). Anal. Calcd for $C_{25}H_{15}Cl_2F_3N_2O$ (%): C, 61.62; H, 3.10; N, 5.75. Found: C, 61.90; H, 3.20; N, 5.61.

4.2. Pharmacology

4.2.1. Materials and animals

Male Sprauge–Dawley rats weighing 250 g were purchased from local source and kept at room temperature (22 ± 2 °C) in a light-controlled room with an alternating 12 h light/dark cycle. They were fasted with free access to water at least 16 h prior to experiments. The tested compounds were prepared as suspension in vehicle (0.5% methyl cellulose) and diclofenac sodium was used as a standard drug. The positive control group animals received the reference drug while the negative control received only the vehicle. An enzyme immunoassay (EIA) kit (catalog number 560101, Cayman Chemical, Ann Arbor, MI, USA) was purchased and used as manufacturer's instructions.

4.2.2. Antiinflammatory activity

The anti-inflammatory activity was evaluated using in vivo rat carrageenan-induced foot paw oedema model reported previously.[34] Oedema was produced by injecting 0.2 mL of a solution of 1% λ-carrageenan in the hind paw. The rats were injected intraperitoneally with 1 mL suspension in 0.5% methyl cellulose of the tested compounds and reference drug. Paw volume was measured by water displacement with a plethysmometer (UGO BASILE) before, 1 and 2 h after treatment. The percentage was calculated by the following equation: anti-inflammatory activity (%) = $(1 - D/C) - 100$, where D represents the difference in paw volume before and after drug was administered to the rats, and C stands for the difference of volume in the control groups.

4.2.3. In vitro cyclooxygenase (COX) inhibition assay

The ability of the test compounds to inhibit ovine COX-1 and COX-2 was determined using an enzyme immunoassay (EIA) (kit catalog number 560101, Cayman Chemical, Ann Arbor, MI, USA) according to the manufacturer's instructions.[35] Cyclooxygenase

catalyzes the first step in the biosynthesis of arachidonic acid (AA) to PGH_2. $PGF_{2\alpha}$, produced from PGH_2 by reduction with stannous chloride, is measured by enzyme immunoassay (ACE™ competitive EIA). Stock solutions of test compounds were dissolved in a minimum volume of DMSO. Briefly, to a series of supplied reaction buffer solutions (960 μL, 0.1 M Tris–HCl pH 8.0 containing 5 mM EDTA and 2 mM phenol) with either COX-1 or COX-2 (10 μL) enzyme in the presence of heme (10 μL) were added 10 μL of various concentrations of test drug solutions (0.01, 0.1, 1, 10, 50, and 100 μM in a final volume of 1 mL). These solutions were incubated for a period of 5 min at 37 °C after which 10 μL of AA (100 μM) solution were added and the COX reaction was stopped by the addition of 50 μL of 1 M HCl after 2 min. $PGF_{2\alpha}$, produced from PGH_2 by reduction with stannous chloride was measured by enzyme immunoassay. This assay is based on the competition between PGs and a PG-acetylcholinesterase conjugate (PG tracer) for a limited amount of PG antiserum. The amount of PG tracer, that is, able to bind to the PG antiserum is inversely proportional to the concentration of PGs in the wells since the concentration of PG tracer is held constant while the concentration of PGs varies. This antibody–PG complex binds to a mouse anti-rabbit monoclonal antibody that had been previously attached to the well. The plate is washed to remove any unbound reagents and then Ellman's reagent, which contains the substrate to acetylcholine esterase, is added to the well. The product of this enzymatic reaction produces a distinct yellow color that absorbs at 410 nm. The intensity of this color, determined spectrophotometrically, is proportional to the amount of PG tracer bound to the well, which is inversely proportional to the amount of PGs present in the well during the incubation: Absorbance $\propto$ [Bound PG Tracer] $\propto 1/PGs$. Percent inhibition was calculated by the comparison of compound treated to various control incubations. The concentration of the test compound causing 50% inhibition (IC_{50}, μM) was calculated from the concentration–inhibition response curve (duplicate determinations).

4.3. Molecular docking methodology

Docking studies have been performed using MOE 2008.10. With this purpose, crystal structure of both COX-1/flurbiprofen (a nonselective-inhibitor) and COX-2/SC-558 (a selective inhibitor) complexes (PDB codes: 1EQH and 1CX2, respectively) were obtained from the Protein Data Bank in order to prepare both proteins for docking studies. Docking procedure was followed using the standard protocol implemented in MOE 2008.10 and the geometry of resulting complexes was studied using the MOE's Pose Viewer utility.

Acknowledgments

The Authors extend their appreciation to the Deanship of Scientific Research at King Saud University for funding the work through the research group project No. RGP-VPP-163.

References and notes

1. Williams, D. A.; Lemke, T. L. Non-steroidal anti-inflammatory drugs. In *Foye's Principles of Medicinal Chemistry*; Williams, D. A., Ed., 5th ed.; Lippincott Williams & Wilkins, 2002; pp 751–793.
2. Frank, M. M.; Fries, L. F. *Immunol. Today* **1991**, *322*, 12.
3. Collier, H. O. J. *Nature* **1971**, *17*, 232.
4. Cryer, B.; Feldman, M. *Arch. Intern. Med.* **1992**, *152*, 1145.
5. Dannhardt, G.; Kiefer, W. *Eur. J. Med. Chem.* **2001**, *36*, 109.
6. Dannhardt, G.; Kiefer, W.; Krämer, G.; Maehrlein, S.; Nowe, U.; Fiebich, B. *Eur. J. Med. Chem.* **2000**, *35*, 499.
7. Bayly, C. I.; Black, C.; Leger, S.; Ouimet, N.; Ouellet, M.; Percival, M. D. *Bioorg. Med. Chem. Lett.* **1999**, *9*, 307.
8. Patel, C. K.; Rami, C. S.; Panigrahi, B.; Patel, C. N. *J. Chem. Pharm. Res.* **2010**, *2*, 73.
9. Sakya, S. M.; Lundy DeMello, K. M.; Minich, M. L.; Rast, B.; Shavnya, A.; Rafka, R. J.; Koss, D. A.; Cheng, H.; Li, J.; Jaynes, B. H.; Ziegler, C. B.; Mann, D. W.; Petras, C. F.; Seibel, S. B.; Silvia, A. M.; George, D. M.; Lund, L. A.; Denis, S. St.; Hickman, A.; Haven, M. L.; Lynch, M. P. *Bioorg. Med. Chem. Lett.* **2006**, *16*, 288.
10. Lehman, F. S.; Beglinger, C. *Curr. Top. Med. Chem.* **2005**, *5*, 449.
11. McGettigan, P.; Henry, D. *JAMA* **2006**, *296*, 1633.
12. Mason, R. P.; Walter, M. F.; McNulty, H. P.; Lockwood, S. F.; Byun, J.; Day, C. A.; Jacob, R. F. *J. Cardiovasc. Pharmacol.* **2006**, *47*, 7.
13. Kurumbail, R. G.; Stevens, A. M.; Gierse, J. K.; McDonald, J. J.; Stegeman, R. A.; Pak, J. Y.; Miyashiro, D.; Gildehaus, J. M.; Penning, T. D.; Seibert, K.; Isakson, P. C.; Stallings, W. C. *Nature* **1996**, *384*, 644.
14. El-Gamal, M. I.; Bayomi, S. M.; El-Ashry, S. M.; Said, S. A.; Abdel-Aziz, A. A.-M.; Abdel-Aziz, N. I. *Eur. J. Med. Chem.* **2010**, *45*, 1403.
15. Abdel-Aziz, A. A.-M.; ElTahir, K. E. H.; Asiri, Y. A. *Eur. J. Med. Chem.* **2011**, *46*, 1648.
16. Picot, D.; Loll, P. J.; Garavito, R. E. *Nature* **1994**, *367*, 243.
17. Lacy, A.; O'Kennedy, R. *Curr. Pharm. Des.* **2004**, *10*, 3797.
18. Lopez-Gonzalez, J. S.; Prado-Garcia, H.; Aguilar-Cazares, D.; Molina-Guarneros, J. A.; Morales-Fuentes, J.; Mandoki, J. J. *J. Lung Cancer* **2004**, *43*, 275.
19. Reddy, S.N.; Mallireddigari, R.M.; Bell, C.S.; Reddy, P.E.; Ramana, V.M.; In 228th ACS National Meeting, Philadelphia, PA, Aug 22–26, 2004.
20. Kontoyianni, M.; McClellan, L. M.; Sokol, G. S. *J. Med. Chem.* **2004**, *47*, 558.
21. MOE 2008.10 of Chemical Computing Group. Inc.
22. Wang, R.; Lu, Y.; Wang, S. *J. Med. Chem.* **2003**, *46*, 2287.
23. Penning, T. D.; Talley, J. J.; Bertenshaw, S. R.; Carter, J. S.; Collins, P. W.; Docter, S.; Graneto, M. J.; Lee, L. F.; Malecha, J. W.; Miyashiro, J. M.; Rogers, R. S.; Rogier, D. J.; Yu, S. S.; Anderson, G. D.; Burton, E. G.; Cogburn, J. N.; Gregory, S. A.; Koboldt, C. M.; Perkins, W. E.; Seibert, K.; Veenhuizen, A. W.; Zhang, Y. Y.; Isakson, P. C. *J. Med. Chem.* **1997**, *40*, 1347.
24. Meade, E. A.; Smith, W. L.; DeWitt, D. L. *J. Biol. Chem.* **1993**, *268*, 6610.
25. Llorens, O.; Perez, J. L.; Palomer, A.; Mauleon, D. *Bioorg. Med. Chem. Lett.* **1999**, *9*, 2779.
26. Garavito, R. M.; DeWitt, D. L. *Biochem. Biophys. Acta* **1999**, *1441*, 278.
27. El-Azab, A. S.; Al-Omar, M. A.; Abdel-Aziz, A. A.-M.; Abdel-Aziz, N. I.; El-Sayed, M. A.-A.; Aleisa, A. M.; Sayed-Ahmed, M. M.; Abdel-Hamide, S. G. *Eur. J. Med. Chem.* **2010**, *45*, 4188.
28. Halgren, T. A. *J. Comput. Chem.* **1996**, *17*, 490.
29. Umezawa, Y.; Tsuboyama, S.; Takahashi, H.; Uzawa, J.; Nishio, M. *Tetrahedron* **1999**, *55*, 10047.
30. El-Ayaan, U.; Abdel-Aziz, A. A.-M.; Al-Shihry, S. *Eur. J. Med. Chem.* **2007**, *42*, 1325.
31. Selinsky, B. S.; Gupta, K.; Sharkey, C. T.; Loll, P. J. *Biochemistry* **2001**, *40*, 5172.
32. Fustero, S.; Román, R.; Sanz-Cervera, J. F.; Simón-Fuentes, A.; Cuñat, A. C.; Villanova, S.; Murgu, M. *J. Org. Chem.* **2008**, *73*, 3523.
33. Singh, S. P.; Kumar, V.; Aggarwal, R. *J. Heterocycl. Chem.* **2006**, *43*, 1003.
34. Winter, C. A.; Risely, E. A.; Nuss, G. W. *Proc. Soc. Exp. Biol.* **1962**, *111*, 544.
35. Uddin, M. J.; Praveen Rao, P. N.; Knaus, E. E. *Bioorg. Med. Chem.* **2004**, *12*, 5929.